The FASEB Journal article fj.11-202994. Published online April 16, 2012.

The FASEB Journal • Research Communication

Glomerular VEGF resistance induced by PKCδ/SHP-1 activation and contribution to diabetic nephropathy

Akira Mima,*[,1] Munehiro Kitada,*[,1] Pedro Geraldes,[†] Qian Li,* Motonobu Matsumoto,* Koji Mizutani,* Weier Qi,* Chenzhong Li,* Michael Leitges,[‡] Christian Rask-Madsen,* and George L. King*[,2]

*Research Division, Joslin Diabetes Center, Harvard Medical School, Boston, Massachusetts, USA; [†]Department of Medicine, University of Sherbrooke, Sherbrooke, Quebec, Canada; and [‡]The Biotechnology Centre of Oslo, University of Oslo, Oslo, Norway

ABSTRACT **This study characterizes the effect of glucose-induced activation of protein kinase Cδ (PKCδ) and Src homology-2 domain-containing phosphatase-1 (SHP-1) expression on vascular endothelial growth factor (VEGF) actions in glomerular podocytes in cultures and in glomeruli of diabetic rodents. Elevation of glucose levels induced PKCδ and p38 mitogen-activated protein kinase (p38 MAPK) to increase SHP-1 expression, increased podocyte apoptosis, and inhibited VEGF activation in podocytes and glomerular endothelial cells. The adverse effects of high glucose levels can be negated by molecular inhibitors of PKCδ, p38MAPK, and SHP-1 and only partially reduced by antioxidants and nuclear factor-κB (NF-κB) inhibitor. Increased PKCδ activation and SHP-1 expression correlated with loss of VEGF signaling and podocyte numbers in the glomeruli of diabetic rats and mice. In contrast, diabetic PKCδ-knockout (*Prkcd*$^{-/-}$) mice did not exhibit activation of p38 MAPK and SHP-1 or inhibition of VEGF signaling in renal glomeruli. Functionally, diabetic *Prkcd*$^{-/-}$ mice had decreased expressions of TGFβ, VEGF, and extracellular matrix and less albuminuria than diabetic *Prkcd*$^{+/+}$ mice. Hyperglycemia and diabetes can cause glomerular podocyte apoptosis and endothelial dysfunction partly due to increased PKCδ/p38 MAPK activation and the expression of SHP-1 to cause VEGF resistance, independent of NF-κB activation.—Mima, A., Kitada, M., Geraldes, P., Li, Q., Matsumoto, M., Mizutani, K., Qi, W., Li, C., Leitges, M., Rask-Madsen, C., King, G. L. Glomerular VEGF resistance induced by PKCδ/ SHP-1 activation and contribution to diabetic nephropathy. *FASEB J.* 26, 000–000 (2012). www.fasebj.org**

Key Words: podocyte apoptosis · hyperglycemia · VEGFR-2

DIABETES IS THE MOST common cause of chronic kidney disease (CKD; ref. 1). An early abnormality in the development of diabetic nephropathy is podocyte foot process effacement and decreased podocyte number (2), which contributes to the breakdown of the glomerular filtration barrier (3). Kidney biopsies from patients with type 2 diabetes showed that loss of podocytes in diabetic nephropathy may predict the progressive course of the disease (4) and has been described in rodent models of diabetes (5). Hyperglycemia has been reported to induce podocyte apoptosis by inhibiting the actions of endogenous protective factor and the production of toxic metabolites, such as oxidants and advanced glycation end-products (6). Recent findings have suggested that vascular endothelial growth factor (VEGF) could be a key protective factor for renal glomeruli, since VEGF expression increases in the kidney with diabetes, and knocking out VEGF leads to cell death in all glomerular cells forming the renal filtration barrier, resulting in proteinuria and renal failure (7).

We have shown previously that hyperglycemia can activate Src homology-2 domain-containing phosphatase-1 (SHP-1), a tyrosine phosphatase, in the retina, leading to the dephosphorylation and deactivation of platelet-derived growth factor (PDGF) receptors crucial for survival of retinal pericytes (8). Substantial evidence has suggested that abnormal VEGF signaling could be involved in glomerular endothelial dysfunction induced by diabetes (7, 9). However, the relationship among VEGF signaling pathway, podocyte apoptosis,

Abbreviations: Ad, adenovirus; CKD, chronic kidney disease; DMEM, Dulbecco's modified Eagle's medium; DN, dominant negative; eNOS, endothelial nitric oxide synthase; Erk1/2, extracellular signal-regulated kinase 1/2; GFP, green fluorescent protein; NAC, *N*-acetylcysteine; NF-κB, nuclear factor-κB; p38 MAPK, p38 mitogen-activated protein kinase; PDGF, platelet-derived growth factor; PKC, protein kinase C; RBX, ruboxistaurin; RGEC, renal glomerular endothelial cell; SD, Sprague-Dawley; SHP-1, Src homology-2 domain-containing phosphatase-1; siRNA, small-interfering RNA; STZ, streptozotocin; TGF-β, transforming growth factor-β; TUNEL, terminal deoxynucleotidyl transferase deoxyuridine triphosphate nick end labeling; VEGF, vascular endothelial growth factor

[1] These authors contributed equally to this work.

[2] Correspondence: Dianne Nunnally Hoppes Laboratory for Diabetes Complications, Research Division, Joslin Diabetes Center, One Joslin Pl., Boston, MA 02215, USA. E-mail: george.king@joslin.harvard.edu

doi: 10.1096/fj.11-202994

This article includes supplemental data. Please visit *http://www.fasebj.org* to obtain this information.

and endothelial dysfunction in diabetes has yet to be clarified, since questions of podocyte and glomeruli responsiveness to VEGF remain unanswered (9). Here, we have characterized the relationships of protein kinase Cδ (PKCδ) and p38 mitogen-activated protein kinase (MAPK) activation with increased SHP-1 expression and impairment of VEGF signaling in podocytes and renal glomerular endothelial cells (RGECs) *in vitro* and *in vivo*.

MATERIALS AND METHODS

Animal studies

All animal protocols were approved by the Joslin Diabetes Center animal care committee in accordance with the U.S. National Institutes of Health (NIH) guidelines. We used age-matched male Sprague-Dawley (SD) rats (Harlan, Indianapolis, IN, USA) and PKCδ-null (*Prkcd*$^{-/-}$) mice as described previously, with breeding pairs provided by M.L. (10). Diabetes was induced in mice over 5 d by injection of streptozotocin [STZ; 55 μg/g body weight (BW); Sigma, St. Louis, MO, USA] in 0.05 M citrate buffer (pH 4.5) and over 1 d in rats. Glycemic levels > 16.7 mM were considered to indicate diabetes. To investigate VEGF signaling, rats were injected with VEGF-A (1 or 4 ng/g BW; R&D, Minneapolis, MN, USA) or diluents into the vena cava at 2 or 12 wk after diabetes. VEGF infusion was performed 15 min before the harvesting of kidneys. Glomerular and tubular fractions were isolated within 30 min after VEGF infusion.

Isolation of glomeruli

Rat glomeruli were isolated from renal cortex by the sieving method, as described previously (11).

Cell culture and reagents

Podocytes from a conditionally immortalized cell line were cultured as described previously (12) and provided by P. Mundel (University of Heidelberg, Heidelberg, Germany). Glomeruli were isolated from kidneys of SD rats at 6 wk of age under sterile conditions. The digested glomeruli were filtered twice through a 100-μm cell strainer (BD Biosciences, San Jose, CA, USA). After centrifugation, the cells were mixed with sheep anti-rat IgG beads (Invitrogen, Carlsbad, CA, USA) coated with anti-ICAM2 antibody or with streptavidin-coupled beads (Invitrogen) with biotin anti-CD31 (BD Biosciences) at antibody concentration of 3 μg for 1×10^7 beads in 1 ml Dulbecco's modified Eagle's medium (DMEM) containing 0.1% BSA. After 1 h, RGECs were isolated using a MPC-50 magnet (Dynal, Hamburg, Germany). The cells were cultured in 10-cm dishes precoated with rat collagen I (5 mg/cm^2; BD Biosciences) at 37°C in a humidified 5% CO_2 atmosphere. On days 5–7 after seeding, outgrowths of individual glomeruli were detached by trypsin-EDTA (Invitrogen) and were washed with DMEM and subsequently treated with 0.1% collagenase type I (Worthington, Lakewood, NJ, USA) in DMEM containing 0.1% BSA at 37°C for 1 h. Endothelial cell purity >90% was assessed by immunofluorescence staining with CD31 (13).

Adenoviral vector infection

Adenoviral vectors were constructed containing green fluorescent protein (GFP; Ad-GFP) and dominant-negative or wild-type PKC-δ isoforms (Ad-DN PKCδ and Ad-WT PKCδ). These adenoviral vectors were used to infect podocytes reported previously (14).

Small-interfering RNA (siRNA) transfection

Podocytes (1.0×10^5) were seeded into 6-well plates and grown until 60–80% confluent. siRNA for SHP-1 or control siRNA (Santa Cruz Biotechnology, Santa Cruz, CA, USA) was combined with lipofectamine RNAi max transfection (Invitrogen), and the cells were transfected according to the recommended protocol with siRNA. At 24 h after transfection, the cells were exposed to low (5.6 mM) or high (20 mM) glucose for 72 h, stimulated with or without VEGF (R&D), and then lysed for DNA fragmentation and immunoblot analyses. To normalize for the hyperosmolality, parallel cultures were maintained in the presence of 5.6 mM glucose and 14.4 mM D-mannitol. Synthetic siRNAs had the following sequences: SHP-1 siRNA A, ACACAGCAGAAUACAAACUtt, AGUUUGUAUUCUGCUGUGUtt; SHP-1 siRNA B, UGACUGUGGUCAUCUGAAUtt, AUUCAGAUGACCACAGUCAtt; SHP-1 siRNA C, UGAGGCUCAUCUCUAGAGUtt, ACUCUAGAGAUGAGCCUCAtt; SHP-1 siRNA D, GGACAUUUCUUGUGCGUGAtt, UCACGCACAAGAAAUGUCCtt.

DNA fragmentation analysis

DNA fragmentation was measured by quantitation of cytosolic oligonucleosome-bound DNA using ELISA according to the manufacturer's instructions (Roche, Indianapolis, IN, USA).

Measurement of urinary albumin

Albuminuria was measured by Albuwell or Nephrat (Exocell, Philadelphia, PA, USA) from 24 h urine collection housed in individual metabolic cages.

Measurement of VEGF-A

The concentration of VEGF-A in the supernatants was measured by Quantikine ELISA kits (R&D) according to the manufacturer's instructions.

Measurement of glomerular cGMP concentration

Glomerular cGMP concentration was measured using a commercially available enzyme immunoassay (GE Healthcare, Piscataway, NJ, USA) as described previously (15).

Immunoblot analysis

Samples were dissolved in 0.5% Nonidet P-40, used after optimization studies, and immunoprecipitated with VEGFR-2 antibody (Cell Signaling, Beverly, MA, USA) and protein A/G Sepharose beads. Proteins were separated by SDS-PAGE. The blots were subsequently incubated with anti-nephrin (Santa Cruz Biotechnology), anti-PKCβ2 (Santa Cruz Biotechnology), anti-PKCδ (Santa Cruz Biotechnology), anti-extracellular signal-regulated kinase 1/2 (Erk1/2; Cell Signaling, Beverly, MA, USA), anti-phospho-Erk1/2 (Cell Signaling), anti-Akt (Cell Signaling), anti-phospho-Akt (Cell Signaling), anti-endothelial nitric oxide synthase (eNOS; Cell Signaling), anti-phospho-eNOS (Cell Signaling), anti-p38 MAPK (Cell Signaling), anti-phospho-p38 MAPK (Cell Signaling), anti-SHP-1 (Cell Signaling), anti-phospho-SHP-1 (Abcam, Cambridge, MA, USA) anti-VEGFR-2 (Cell Signaling), anti-phospho-VEGFR-2 (Cell Signaling), anti-phospho-IκBα (Cell Signaling), anti-cleaved caspase-3 (Cell Sig-

naling), anti-nephrin (Santa Cruz Biotechnology), anti-phosphonephrin (Abcam), and anti-WT-1 (Santa Cruz Biotechnology). Labeled protein bands were identified with enhanced chemiluminescent system (Amersham Biosciences, Piscataway, NJ, USA). Equal loading was confirmed using anti-actin antibodies (Santa Cruz Biotechnology), anti-p-cadherin (Abcam) or anti-GAPDH (Abcam), and expression was normalized using ImageJ software (NIH, Bethesda, MD, USA).

Real-time PCR analysis

PKCδ, SHP-1, transforming growth factor-β (TGF-β), Col4, VEGF, and VEGFR-2 were assayed by real-time PCR and normalized to 18S rRNA. PCR primers were mouse, PKCδ TTCCTGCGCATCTCCTTCA, AAAGGCTGGCTTGCTTCGT; rat, PKC-δ TCCTGCGCATCTCCTTCAATTCCT, ACATGGTGGGCTTCTTCTGTACCA; mouse, SHP-1 TGGTTTCACCGGGACCTCAGC, AGTAAGGGTGCCGCAGGTAGA; rat, SHP-1 ATCAACCAGCGGCAGGAAAGTTTG, ATCAATGATGATGATGGTGCCCGT; TGF-β, TGCTTCAGCTCCACAGAGAA, TGGTTGTAGAGGGCAAGGAC; Col4, GCCAAGTGTGCATGAGAAGA, AGCGGGGTGTGTTAGTTACG; VEGF, CTCGCAGTCCGAGCCGGAGA, GGTGCAGCCTGGGACCACTTG; VEGFR-2, ATGTGAAGCCATCAACAAAGCGGG, GGGCAGCAGGTTGCACAGTAATTT.

Immunohistochemistry, terminal deoxynucleotidyl transferase deoxyuridine triphosphatenick end labeling (TUNEL), and enumeration of podocytes

Kidney sections were processed for immunohistochemistry as previously published (13). Sections were fixed in acetone, blocked with donkey serum, and incubated with antibodies as indicated. Apoptotic cells were detected using the ApopTag Plus kit (Chemicon, Temecula, CA, USA). Podocyte counting was performed on glomerular sections immunostained with WT-1 (Santa Cruz Biotechnology). Glomeruli were digitally photographed, and the images were imported into ImageJ software (NIH) and analyzed morphometrically. The estimated average number of podocytes per glomerulus was determined by the stereologic method, as reported previously (4, 16, 17).

Measurement of PKC activity assay and immunoblot analysis

To evaluate PKC activity in the cultured podocytes, a modified *in situ* PKC assay was used, as described previously (8).

Reagents

SB203580 and SN50 were purchased from Calbiochem. VEGF-A neutralizing antibody was purchased from R&D. *N*-acetylcystein (NAC) was purchased from Sigma. PKCβ-selective inhibitor ruboxistaurin (RBX; LY333531) was provided by Lilly (Indianapolis, IN, USA).

Data analysis

The data are expressed as means ± SD. Comparisons were made between groups using either 2-sample and paired *t* tests for 2-way comparisons, or 1-way ANOVA for multiple groups to establish statistically significant differences. All analyses were performed using StatView (SAS Institute, Cary, CA, USA). Statistical significance was defined as $P < 0.05$.

RESULTS

Effect of glucose on PKCδ activation and VEGF signaling

High glucose (20 mM) levels increased *in situ* PKC activity by 1.5 ± 0.3-fold in podocytes (Supplemental Fig. S1*A*). Immunoblot analyses showed that high glucose levels increased the levels of the PKCα, PKCβ2, and PKCδ isoforms in membrane fractions of podocytes by 1.7 ± 0.1, 2.4 ± 1.4, and 2.6 ± 0.3-fold, respectively, when compared to low-glucose (5.6 mM) conditions (Supplemental Fig. S1*B*). Levels of PKCε and PKCζ isoforms were not changed by high-glucose conditions (data not shown).

To determine whether PKCδ can cause podocyte apoptosis due to the effects of glucose elevation, podocytes were infected with adenoviral vectors expressing GFP (Ad-GFP), dominant-negative (Ad-DN), or wild-type (Ad-WT) PKCδ isoforms. Infection with Ad-DN PKCδ did not affect the activation of PKCα or PKCβ2 (Supplemental Fig. S1*C*). Podocytes infected with Ad-GFP responded to high glucose with a 1.8 ± 0.2-fold increase in DNA fragmentation compared to controls (**Fig. 1*A***). Infection with Ad-WT PKCδ alone but not Ad-WT PKCα or Ad-WT PKCβ2 increased DNA fragmentation by 1.4 ± 0.1- and 2.2 ± 0.1-fold in low- and high-glucose conditions, respectively (Fig. 1*A* and Supplemental Fig. S1*C*). Infection with Ad-DN PKCδ reduced the effects of high glucose on DNA fragmentation by 38 ± 2% (Fig. 1*A*). Further, the PKCβ-selective inhibitor RBX (LY333531) did not affect high-glucose-induced increase in DNA fragmentation (Supplemental Fig. S1*D*).

Podocytes exposed to high-glucose conditions for 72 h increased DNA fragmentation by 1.8 ± 0.2-fold compared to low-glucose conditions (Fig. 1*B*); this effect was reduced by 41 ± 2% by the addition of VEGF-A (Fig. 1*B*). However, VEGF-A did not decrease DNA fragmentation in high-glucose conditions (Fig. 1*B*). The addition of VEGF-neutralizing antibody or SU1498, a VEGFR-2 inhibitor, abolished VEGF-A anti-apoptotic actions totally (Fig. 1*B*). Elevating glucose levels in the medium from 5.6 to 20 mM increased VEGF-A levels in podocyte culture medium in a time-dependent manner as compared to low-glucose conditions by 1.5 ± 0.2-fold; 72 h (Fig. 1*C*).

Effects of high glucose levels on PKCδ, p38 MAPK, and VEGF-A signaling

In low-glucose conditions, VEGF-A (50 ng/ml) activated p-Akt and p-Erk1/2 in podocytes by 4.0 ± 0.2-fold and 5.3 ± 0.2-fold, respectively (Fig. 1*D*, *E*). These effects of VEGF-A were decreased by 62 ± 11% (p-Akt) and by 52 ± 8% (p-Erk1/2) in Ad-GFP-infected podocytes when exposed to high-glucose conditions (Fig. 1*D*, *E*). Further, podocytes infected with Ad-WT PKCδ impaired VEGF-A-induced phosphorylation of Akt by 59 ± 11% and Erk1/2 by 63 ± 10% at low glucose concentrations, respectively (Fig. 1*D*, *E*). Lastly, in cells infected with Ad-DN PKCδ, the inhibiting effects of high glucose on VEGF signaling were completely prevented (Fig. 1*D*, *E*).

Since p38 MAPK activation (p-p38 MAPK) induced by

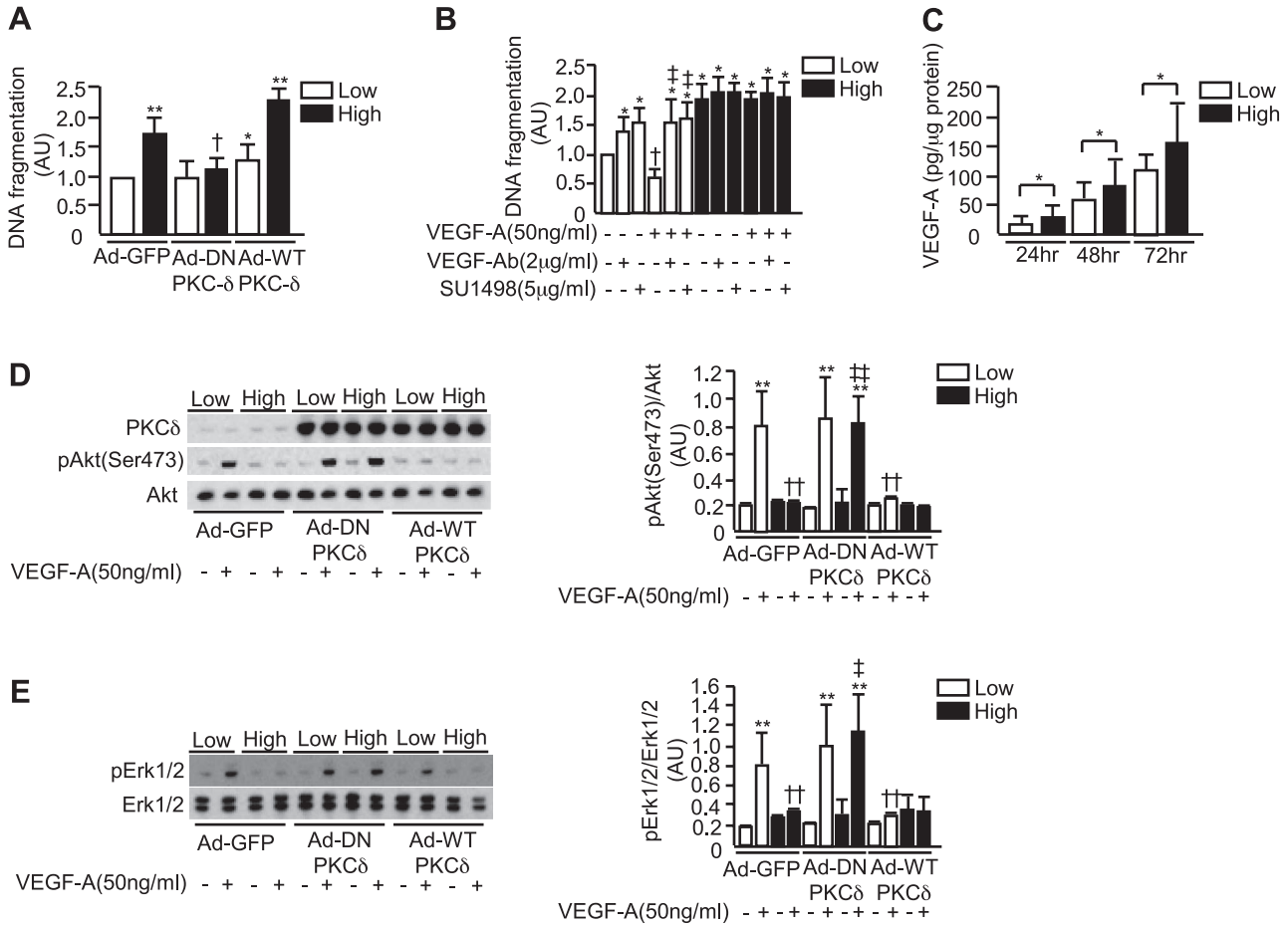

Figure 1. Effects of high glucose levels on VEGF signaling in cultured podocytes. *A*) DNA fragmentation in podocytes infected with Ad-GFP, Ad-DN PKCδ, or Ad-WT PKCδ as indicated and incubated with low glucose (5.6 mM; low) or high glucose (20 mM; high) for 72 h. $^{*}P < 0.05$, $^{**}P < 0.001$ *vs.* low/Ad-GFP. $^{\dagger}P < 0.05$ *vs.* high/Ad-GFP. *B*) DNA fragmentation in podocytes incubated with low glucose or high glucose for 72 h in the absence or presence of VEGF-A (50 ng/ml), VEGF-Ab (2 μg/ml), and SU1498 (5 μg/ml). $^{*}P < 0.05$ *vs.* low/VEGF-A(−)/VEGF-Ab(−)/SU1498(−). $^{\dagger}P < 0.05$ *vs.* low/VEGF-A(−)/VEGF-Ab(−)/SU1498(−). $^{\ddagger}P < 0.05$ *vs.* low/VEGF-A(+)/VEGF-Ab(−)/SU1498(−). *C*) After 24–72 h of exposure to low glucose or high glucose, VEGF-A levels in the culture medium were measured with the VEGF-A assay kit. $^{*}P < 0.05$. *D*, *E*) Immunoblot analyses of phosphor-Akt (*D*), Akt (*D*), phosphor-Erk1/2 (*E*), and Erk1/2 (*E*) and densitometric quantification with or without addition of VEGF-A (50 ng/ml). $^{**}P < 0.001$ *vs.* low/VEGF-A(−)/Ad-GFP. $^{\dagger\dagger}P < 0.001$ *vs.* low/VEGF-A(+)/Ad-GFP. $^{\ddagger}P < 0.05$, $^{\ddagger\ddagger}P < 0.001$ *vs.* high/VEGF-A(+)/Ad-GFP. Data are expressed as means ± SD; $n = 4–6$; 1 of 3 independent experiments is shown.

PKCδ can cause apoptosis of cells, including pericytes (8, 18, 19), we explored its involvement in high-glucose-dependent inhibition of VEGF signaling. High glucose levels increased p38 MAPK phosphorylation in podocytes by 1.9 ± 0.1-fold (Supplemental Fig. S1*E*). p38 MAPK selective inhibitor SB203580 reduced high-glucose-induced podocyte apoptosis by 32 ± 4% (Supplemental Fig. S1*F*). Lastly, high glucose levels inhibited VEGF-A-induced p-Akt and p-Erk1/2 by 77 ± 5 and 57 ± 5%, respectively; this effect was reversed by the addition of SB203580, a p38 MAPK inhibitor (Supplemental Fig. S1*G*, *H*).

Role of SHP-1 and nuclear factor-κB (NF-κB) activation on VEGFR-2 signaling cascade

Since SHP-1 is a downstream target of PKCδ and p38 MAPK activation in pericytes (8), we evaluated its role on glucose-induced inhibition of VEGF actions in podocytes. After 3 d of high-glucose incubation, SHP-1 expression was increased in podocytes by 27 ± 10% (**Fig. 2*A***). The effect of PKCδ and p38 MAPK activation on SHP-1 expression induced by high glucose was studied using SB203580, or Ad-WT PKCδ and Ad-DN PKCδ. High glucose-induced SHP-1 protein expression was reduced by 14 ± 2% when podocytes were preincubated with SB203580 (Supplemental Fig. S1*I*). Infection with Ad-WT PKCδ increased SHP-1 protein expression by 1.7 ± 0.2-fold compared to infection with Ad-GFP (Fig. 2*B*). In contrast, infection with Ad-DN PKCδ reduced the effects of high glucose on SHP-1 protein expression by 45 ± 5% (Fig. 2*B*). Further, infection with Ad-WT PKCδ increased phosphorylation of SHP-1 by 1.4 ± 0.2-fold compared to infection with Ad-GFP (Fig. 2*C*).

High glucose levels (20 mM) induced phosphorylation of p38 MAPK by 2.2 ± 0.4-fold compared to low glucose (5.6 mM) (Supplemental Fig. S1*J*). When podo-

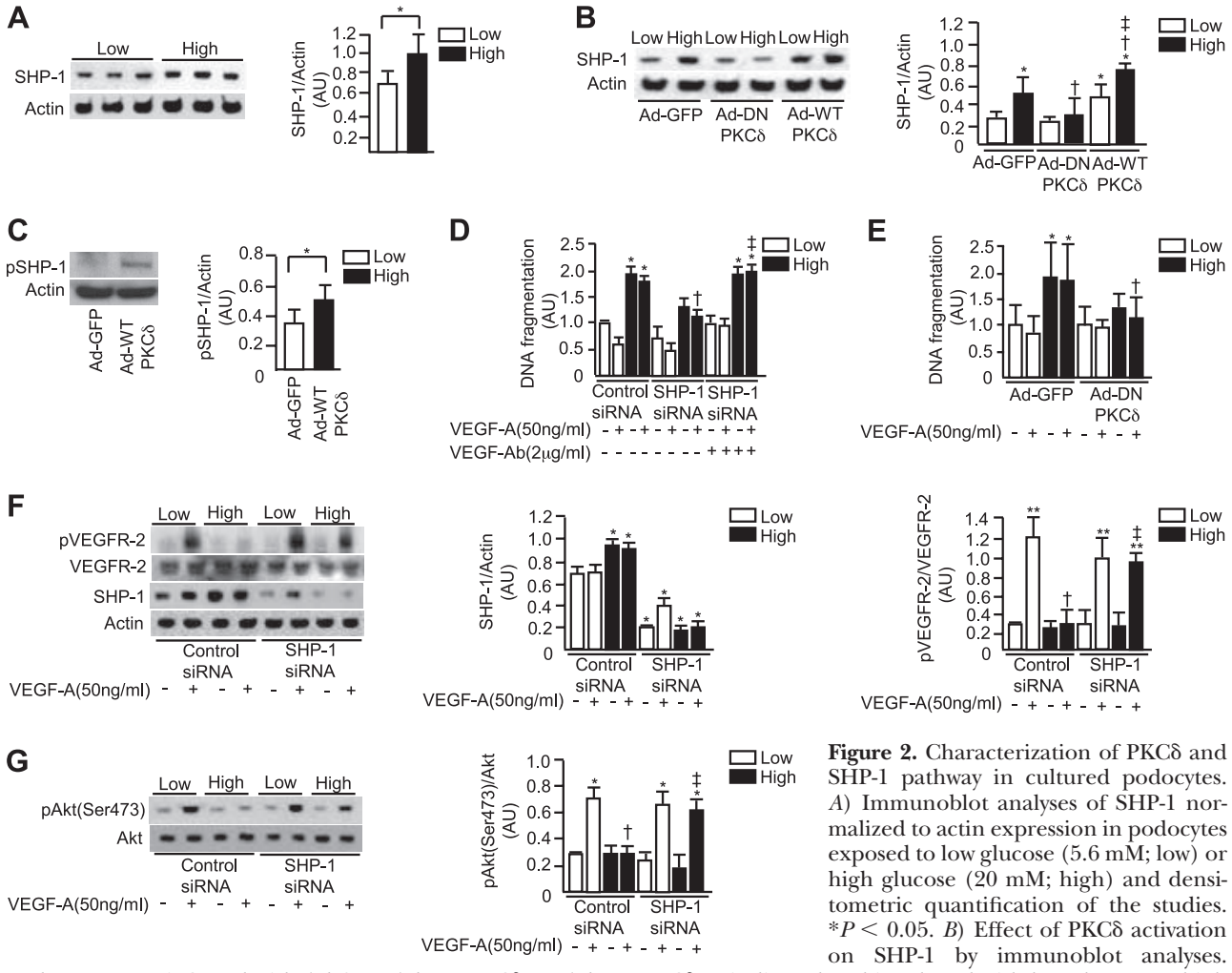

Figure 2. Characterization of PKCδ and SHP-1 pathway in cultured podocytes. *A*) Immunoblot analyses of SHP-1 normalized to actin expression in podocytes exposed to low glucose (5.6 mM; low) or high glucose (20 mM; high) and densitometric quantification of the studies. $^{*}P < 0.05$. *B*) Effect of PKCδ activation on SHP-1 by immunoblot analyses. Podocytes were infected with Ad-GFP, Ad-DN PKCδ, or Ad-WT PKCδ as indicated and incubated with low glucose or high glucose for 72 h. $^{*}P < 0.05$ *vs.* low/Ad-GFP. $^{\dagger}P < 0.05$ *vs.* high/Ad-GFP. $^{\ddagger}P < 0.05$ *vs.* low/Ad-WT PKCδ. *C*) Effect of PKCδ activation on phosphorylation of SHP-1 by immunoblot analyses. Podocytes were infected with Ad-GFP or Ad-WT PKCδ as indicated. $^{*}P < 0.05$. *C*) Effect of SHP-1 and VEGF on glucose-induced apoptosis, as measured by DNA fragmentation. Podocytes were transfected with the indicated siRNA and then incubated with low glucose or high glucose in the presence or absence of VEGF-A (50 ng/ml) or VEGF-Ab (2 μg/ml). $^{*}P < 0.05$ *vs.* low/control siRNA/VEGF-A(−)/VEGF-Ab(−). $^{\dagger}P < 0.05$ *vs.* high/control siRNA/VEGF-A(+)/VEGF-Ab(−). $^{\ddagger}P < 0.05$ *vs.* high/SHP-1 siRNA/VEGF-A(+)/VEGF-Ab(−). *D*) Effect of PKCδ and VEGF on glucose-induced apoptosis, as measured by DNA fragmentation. Podocytes were infected with Ad-GFP or Ad-DN PKCδ as indicated and incubated with low glucose or high glucose in the presence or absence of VEGF-A (50 ng/ml). $^{*}P < 0.05$ *vs.* low/Ad-GFP/VEGF-A(−). $^{\dagger}P < 0.05$ *vs.* high/Ad-GFP/VEGF-A(+). *E, F*) Immunoblot analyses of SHP-1 (*E*), phospho-VEGFR-2 (*E*) and phospho-Akt (*F*) in podocytes transfected with the indicated siRNA, exposed to low glucose mM) or high glucose. $^{*}P < 0.05$, $^{**}P < 0.001$ *vs.* low/control siRNA/VEGF-A(−). $^{\dagger}P < 0.05$ *vs.* low/control siRNA/VEGF-A(+). $^{\ddagger}P < 0.05$ *vs.* high/control siRNA/VEGF-A(+). Data are expressed as means ± SD; n = 4–6; 1 of 3 independent experiments is shown.

cytes incubated in high-glucose conditions were infected with Ad-DN-PKCδ, p38 MAPK phosphorylation was significantly inhibited by 43 ± 2% (Supplemental Fig. S1*J*). Infection with Ad-WT PKCδ increased p-PKCδ and p-p38 MAPK by 9.8 ± 2.1- and 2.4 ± 0.3-fold, respectively, and SHP-1 protein levels by 1.7 ± 0.6-fold (Supplemental Fig. S1*K*). However, levels of p-p38 MAPK and SHP-1 did not increase when the cells were infected with Ad-WT PKCα or Ad-WT PKCβ2 (Supplemental Fig. S1*K*).

To assess the role of SHP-1 in mediating the effect of hyperglycemia on podocyte apoptosis, SHP-1 expression was reduced with siRNA. SiRNA of SHP-1 reduced protein levels of SHP-1 by 50 ± 5 to 76 ± 3% (Fig. 2*E*), which reduced high-glucose-induced apoptosis by 35 ± 2% (Fig. 2*D*). However, VEGF-A-neutralizing antibody also reduced the protective actions of SHP-1 siRNA significantly (Fig. 2*D*). Similarly, knockdown of PKCδ with Ad-PKCδ in podocytes inhibited high-glucose-induced apoptosis by 41 ± 5% (Fig. 2*E*). Podocytes exposed to high-glucose conditions inhibited VEGF-A signaling actions compared to low-glucose conditions as measured by p-VEGFR-2 (77±10%), p-Akt (45±11%), and p-Erk1/2 (53±10%) (Fig. 2*F, G* and Supplemental Fig. S1*L*). In contrast, knockdown of SHP-1 with siRNA in podocytes significantly restored these signaling actions of VEGF in high-glucose conditions (Fig. 2*F, G* and Supplemental Fig. S1*L*).

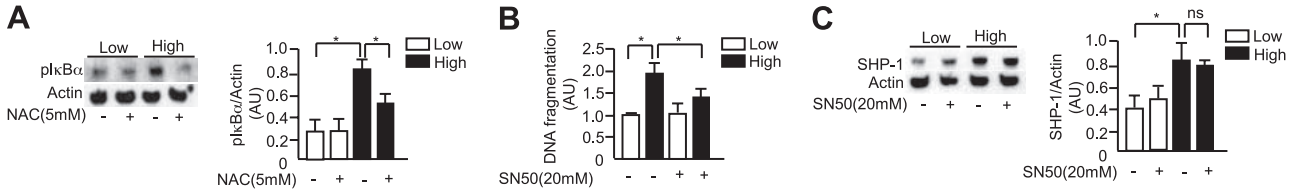

Figure 3. Evaluation of SHP-1 and antioxidants on high-glucose-induced VEGF signaling pathway. *A*) Effect of glucose and NAC on phospho-IκBα by immunoblot analysis. Podocytes were incubated with low glucose (5.6 mM) or high glucose (20 mM) for 72 h in the absence or presence of NAC (5 mM). *B*) Effect of NF-κB inhibition on glucose-induced apoptosis. DNA fragmentation in podocytes incubated with low glucose or high glucose for 72 h in the absence or presence of SN50 (20 mM). $*P < 0.05$. *C*) Immunoblot analyses of SHP-1 in low and high glucose and NF-κB inhibition. Podocytes were incubated with low glucose or high glucose for 72 h in the absence or presence of SN50 (20 mM). ns, not significant. Data are expressed as means ± SD; $n = 3–4$; 1 of 3 independent experiments is shown. $*P < 0.05$.

NF-κB activation was studied due to its reported involvement in pericyte and podocyte apoptosis induced by hyperglycemia and diabetes (20). Incubation in high-glucose conditions increased phosphorylation of IκBα by 4.6 ± 1.8-fold compared to low-glucose conditions in podocytes (**Fig. 3*A***). The addition of NAC prevented this activation by 39 ± 4% (Fig. 3*A*). Selective inhibitor of NF-κB translocation to the nucleus SN50 only reduced high-glucose-induced DNA fragmentation by 29 ± 5% (Fig. 3*B*) and did not prevent the induction of SHP-1 expression by high-glucose conditions (Fig. 3*C*).

Effect of diabetes on VEGF-A signaling in the glomeruli

After 12 wk of diabetes, blood glucose levels increased by 4.4 ± 0.6-fold and kidney weight per body weight increased by 2.1 ± 0.2-fold in diabetic SD rats compared to nondiabetic controls (**Table 1**). Glomerular expression of nephrin and WT-1 were decreased by 29 ± 8 and 38 ± 12%, respectively, compared to nondiabetic SD rats (**Fig. 4*A***). The glomerular levels of apoptotic marker cleaved caspase-3 normalized to nephrin by dual immunal labeling was increased in diabetic SD rats by 13 ± 5-fold compared to nondiabetic SD rats (Fig. 4*B*).

Double immunostaining of renal glomeruli for VEGFR-2 and nephrin showed the presence of VEGFR-2 in podocytes (Supplemental Fig. S2*A*). The effect of diabetes on VEGF-A to activate Akt (p-Akt), eNOS phosphorylation (p-eNOS), Erk1/2 (p-Erk1/2), and nephrin (p-nephrin) phosphorylation in the renal glomeruli were studied. After 2 wk of diabetes, infusion of VEGF-A (1 ng/g BW) into inferior vena cava increased the levels of p-Akt, p-eNOS, and p-Erk1/2 in the whole glomeruli of nondiabetic SD rats by 6.6 ± 0.8-, 5.9 ± 0.2-, and 5.1 ± 0.2-fold, respectively, (Fig. 4*C*, *D*); this effect was reduced in diabetic SD rats by 29 ± 12, 43 ± 8, and 36 ± 3%, respectively. In contrast, when the rats were given high doses of VEGF-A (4 ng/g BW), diabetes did not inhibit the effects of VEGF action on p-Akt, p-eNOS, and p-Erk1/2 (Fig. 4*C*, *D*). Infusion of VEGF-A (1 ng/g BW) at low doses increased p-nephrin by 8.0 ± 0.9-fold in nondiabetic SD rats but inhibited p-nephrin by 32 ± 9% in diabetic SD rats (Fig. 4*E*). Even at high doses of VEGF-A (4 ng/g BW), diabetes still inhibited VEGF induction of p-nephrin, significantly, by 20 ± 3% (Fig. 4*E*). In contrast, after 12 wk of diabetes, VEGF-A (1 ng/g BW)-induced phosphorylation of p-Akt, p-eNOS, p-Erk, and p-nephrin was significantly more inhibited compared to 2 wk of diabetes (p-Akt by 57±6%, p-eNOS by 58±12%, p-Erk by 57±3%, and p-nephrin by 51±9%, Fig. 4*F–H*). Further, VEGF-induced cGMP production in the glomeruli was significantly decreased in diabetic SD rats by 72 ± 11%, compared to nondiabetic SD rats (Fig. 4*I*).

TABLE 1. *General characteristics of experimental groups*

Characteristic	Rat group	
	NDM SD	DM SD
Number	6	6
Body weight (g)	567 ± 37	393 ± 50*
Blood glucose (mg/dl)	98 ± 9	427 ± 76**
rKW/BW (mg/g)	6.1 ± 0.3	13.3 ± 1.4**
UAE (mg/d)	0.4 ± 0.1	4.6 ± 2.2*

NDM SD, nondiabetic model Sprague-Dawley; DM SD, diabetic model Sprague-Dawley; rKW/BW, right kidney weight/body weight; UAE, urinary albumin excretion. Data are expressed as means ± SD $*P < 0.05$, $**P < 0.001$ *vs.* NDM SD.

Effect of high glucose levels on VEGF-A signaling in podocytes and RGECs

VEGF-A (50 ng/ml) increased p-nephrin by 1.8 ± 0.4-fold in podocytes; however, when the podocytes were incubated with high glucose, the VEGF effect was decreased by 38 ± 12% (**Fig. 5*A***). Moreover, exogenous VEGF-A increased VEGF mRNA expression by 2.2 ± 0.2-fold and that of VEGFR-2 by 1.9 ± 0.8-fold, respectively; this effect was blunted by 28 ± 3 and 20 ± 9% when the cells were incubated with high glucose (Fig. 5*B*). We also characterized VEGF action in RGECs. As shown in Fig. 5*C*, VEGF-A increased p-VEGFR-2, p-Akt, and p-eNOS levels in a dose-dependent manner (0, 1, 2, 5, 10, 50 ng/ml), reaching a maximum effect at 10 ng/ml, with significant increases of p-VEGFR-2 by 3.6 ± 0.8-fold, p-Akt by 3.3 ± 0.3-fold, and p-eNOS by 5.9 ± 0.2-fold. In high-glucose conditions, VEGF-A (5 ng/ml)-induced p-VEGFR-2, p-Akt, and p-eNOS were decreased by 18 ± 7, 17 ± 6, and 12 ± 4%, respectively. In contrast, high glucose did not inhibit VEGF signaling at 10 and 50 ng/ml (Fig. 5*C*). Similarly, VEGF-A

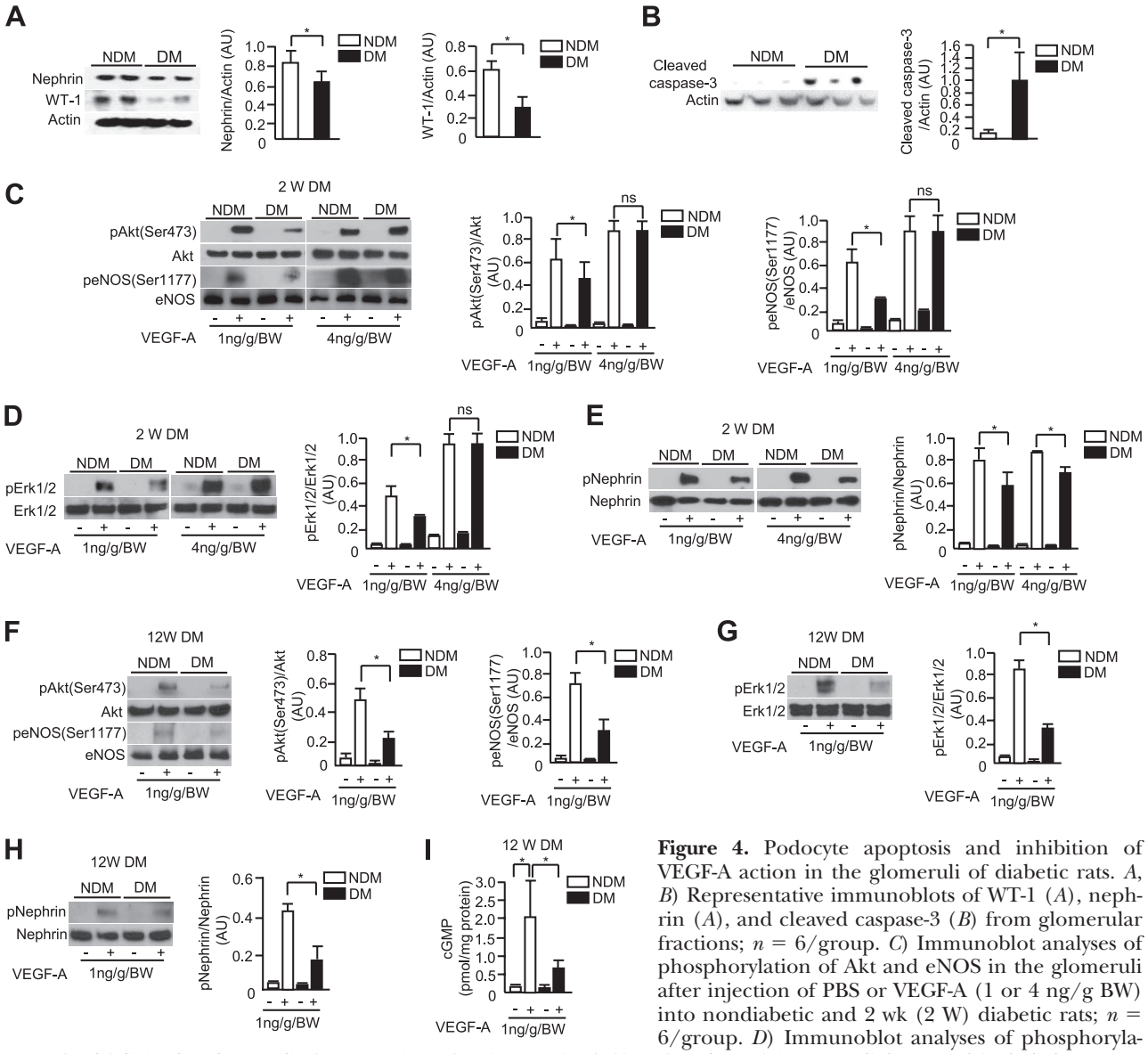

Figure 4. Podocyte apoptosis and inhibition of VEGF-A action in the glomeruli of diabetic rats. *A*, *B*) Representative immunoblots of WT-1 (*A*), nephrin (*A*), and cleaved caspase-3 (*B*) from glomerular fractions; $n = 6$/group. *C*) Immunoblot analyses of phosphorylation of Akt and eNOS in the glomeruli after injection of PBS or VEGF-A (1 or 4 ng/g BW) into nondiabetic and 2 wk (2 W) diabetic rats; $n = 6$/group. *D*) Immunoblot analyses of phosphorylation of Erk1/2 in the glomeruli after injection of PBS or VEGF-A (1 or 4 ng/g BW) into nondiabetic and 2 wk diabetic rats; $n = 6$/group. *E*) Immunoblot analyses of phosphorylation of nephrin in the glomeruli injection of PBS or VEGF-A (1 or 4 ng/g BW) into nondiabetic and 2 wk diabetic rats; $n = 6$/group. *F*) Immunoblot analyses of phosphorylation of Akt and eNOS in the glomeruli after injection of PBS or VEGF-A (1 ng/g BW) into nondiabetic and 12 wk (12 W) diabetic rats; $n = 3$ for nondiabetic group, $n = 4$ for diabetic group. *G*) Immunoblot analyses of phosphorylation of Erk1/2 in the glomeruli after injection of PBS or VEGF-A (1 ng/g BW) into nondiabetic and 12 wk diabetic rats; $n = 3$ for nondiabetic group, $n = 4$ for diabetic group. *H*) Immunoblot analyses of phosphorylation of nephrin in the glomeruli injection of PBS or VEGF-A (1 ng/g BW) into nondiabetic and 12 wk diabetic rats; $n = 3$ for nondiabetic group, $n = 4$ for diabetic group. *I*) cGMP concentration was measured in lysate of glomeruli; $n = 3$ for nondiabetic group, $n = 4$ for diabetic group. DM, STZ-induced diabetic model group; NDM, nondiabetic model group; ns, not significant. Data are expressed as means ± SD; 1 of 3 independent experiments is shown. $^*P < 0.05$.

increased p-Erk1/2 in a dose-dependent manner and reached maximum at 10 ng/ml by 7.9 ± 0.2-fold (Fig. 5*D*). In high-glucose conditions, VEGF induction of p-Erk1/2 was decreased by 14 ± 7% (VEGF-A; 5 ng/ml, Fig. 5*D*) but not inhibited at VEGF-A levels of 10 and 50 ng/ml (Fig. 5*D*).

The effects of VEGF signaling and action in RGECs with or without angiotensin II (AngII) in high-glucose conditions were studied since AngII has also been shown to enhance the toxic effects of hyperglycemia. VEGF-A-induced increases of p-VEGFR-2, p-Akt, and p-eNOS were significantly inhibited in high-glucose conditions with Ang II by 66 ± 2, 64 ± 2, and 57 ± 3%, respectively, compared to low glucose without Ang II (Fig. 5*E*) or high glucose alone.

Expression of SHP-1 and p38 MAPK in the glomeruli of diabetic rats

SHP-1 protein expression was increased in the glomeruli of diabetic SD rats by 2.1 ± 0.9-fold after 3 mo of diabetes in parallel with increases of PKCδ levels by 1.9 ± 0.4-fold

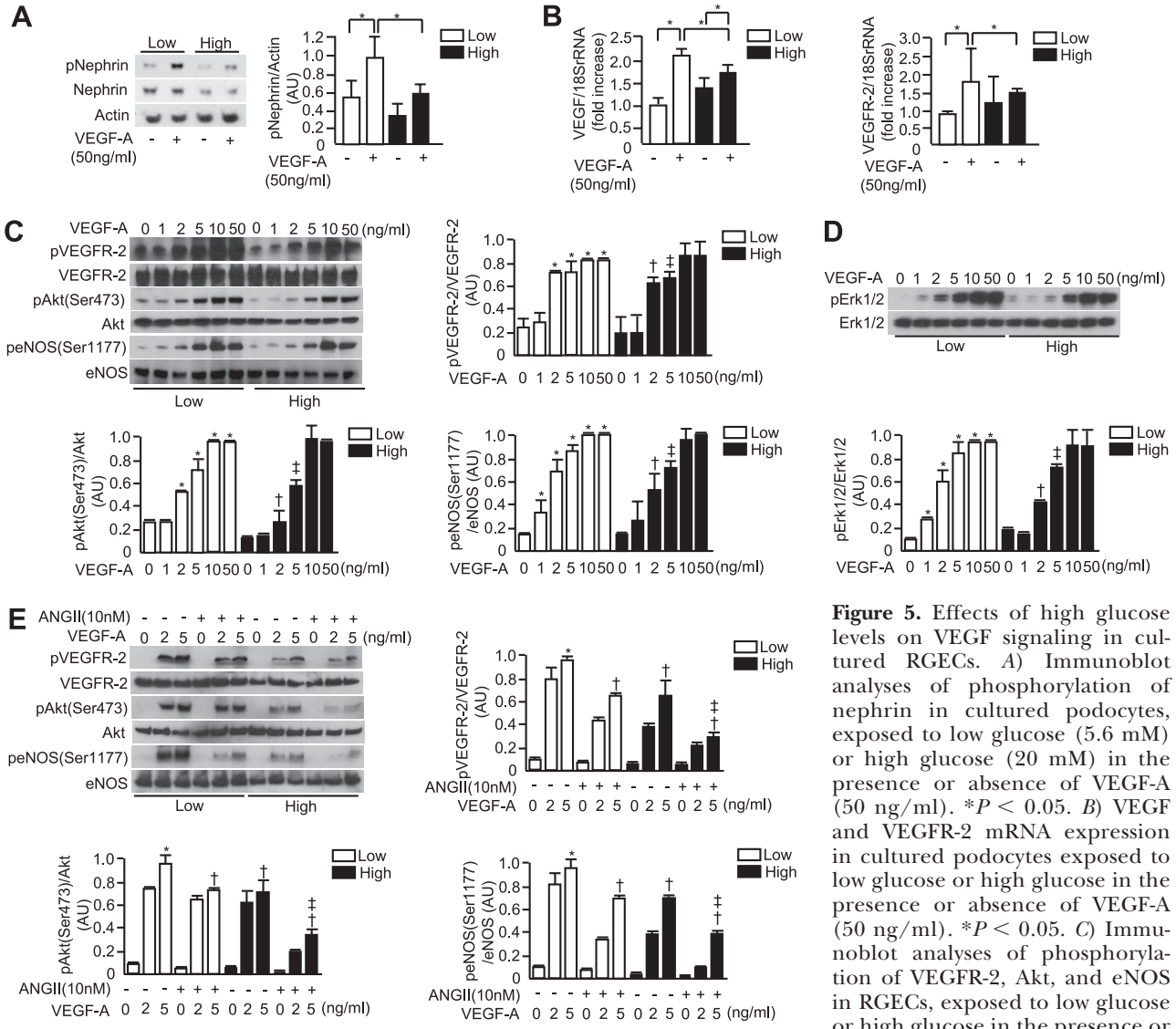

Figure 5. Effects of high glucose levels on VEGF signaling in cultured RGECs. *A*) Immunoblot analyses of phosphorylation of nephrin in cultured podocytes, exposed to low glucose (5.6 mM) or high glucose (20 mM) in the presence or absence of VEGF-A (50 ng/ml). $^*P < 0.05$. *B*) VEGF and VEGFR-2 mRNA expression in cultured podocytes exposed to low glucose or high glucose in the presence or absence of VEGF-A (50 ng/ml). $^*P < 0.05$. *C*) Immunoblot analyses of phosphorylation of VEGFR-2, Akt, and eNOS in RGECs, exposed to low glucose or high glucose in the presence or absence of VEGF-A as indicated. $^*P < 0.05$ *vs.* low/VEGF-A(−). $^\dagger P < 0.05$ *vs.* low/VEGF-A(2 ng/ml). $^\ddagger P < 0.05$ *vs.* low/VEGF-A(5 ng/ml). *D*) Immunoblot analyses of phosphorylation of Erk1/2 in RGECs, exposed to low glucose or high glucose in the presence or absence of VEGF-A as indicated. $^*P < 0.05$ *vs.* low/VEGF-A(−). $^\dagger P < 0.05$ *vs.* low/VEGF-A(2 ng/ml). $^\ddagger P < 0.05$ *vs.* low/VEGF-A(5 ng/ml). Data are expressed as means ± SD; $n = 4$; 1 of 3 independent experiments is shown.

and p-p38 MAPK by 2.8 ± 0.1-fold (**Fig. 6*A*** and Supplemental Fig. S2*B*). However, only the expression of SHP-1 and PKCδ mRNA levels were increased in the glomeruli of SD diabetic rats, by 1.5 ± 0.3- and 1.3 ± 0.1-fold, respectively (Fig. 6*B*). Expression of PKCδ protein levels were also increased at 1 mo of diabetes (Supplemental Fig. S2*C*). Immunohistochemistry study showed that SHP-1 expression overlapped significantly with synaptopodin, and its expression was increased mainly in the glomeruli of diabetic SD rats compared to control SD rats (Fig. 6*C*).

Effect of diabetes on SHP-1 activation and podocyte apoptosis in *Prkcd*$^{-/-}$ mice

Since PKCδ activation can induce apoptosis in cultured podocytes, we examined the changes in p38 MAPK and SHP-1 expression in the glomeruli of nondiabetic and diabetic *Prkcd*$^{-/-}$ and age-matched *Prkcd*$^{+/+}$ mice. After 6 mo of diabetes, diabetic *Prkcd*$^{+/+}$ and *Prkcd*$^{-/-}$ mice exhibited similar reductions in body weight, compared to nondiabetic *Prkcd*$^{+/+}$ mice (by 30±9 *vs.* 32±10% in *Prkcd*$^{+/+}$ *vs. Prkcd*$^{-/-}$ mice; **Table 2**). Histological analyses of the glomeruli showed that diabetes decreased podocyte density as measured by Weibel-Gomez method in diabetic compared to nondiabetic *Prkcd*$^{+/+}$ mice. However, the effect of diabetes was reduced significantly in diabetic *Prkcd*$^{-/-}$ mice (by 55±12 *vs.* 32±14% in *Prkcd*$^{+/+}$ *vs. Prkcd*$^{-/-}$ mice; **Fig. 7*A***). Histological analyses of the glomeruli also showed that diabetes increased cleaved caspase-3/nephrin/DAPI triple-positive cells by 10 ± 4-fold compared to nondiabetic *Prkcd*$^{+/+}$ mice, and this effect was reduced by 41 ± 20% in diabetic *Prkcd*$^{-/-}$ mice (Fig. 7*B*). Similarly, protein expression of cleaved caspase-3 in the renal cortex was elevated in diabetic *Prkcd*$^{+/+}$ mice by 8.6 ± 1.3-fold compared to nondiabetic *Prkcd*$^{+/+}$ mice. However, the increases in cleaved

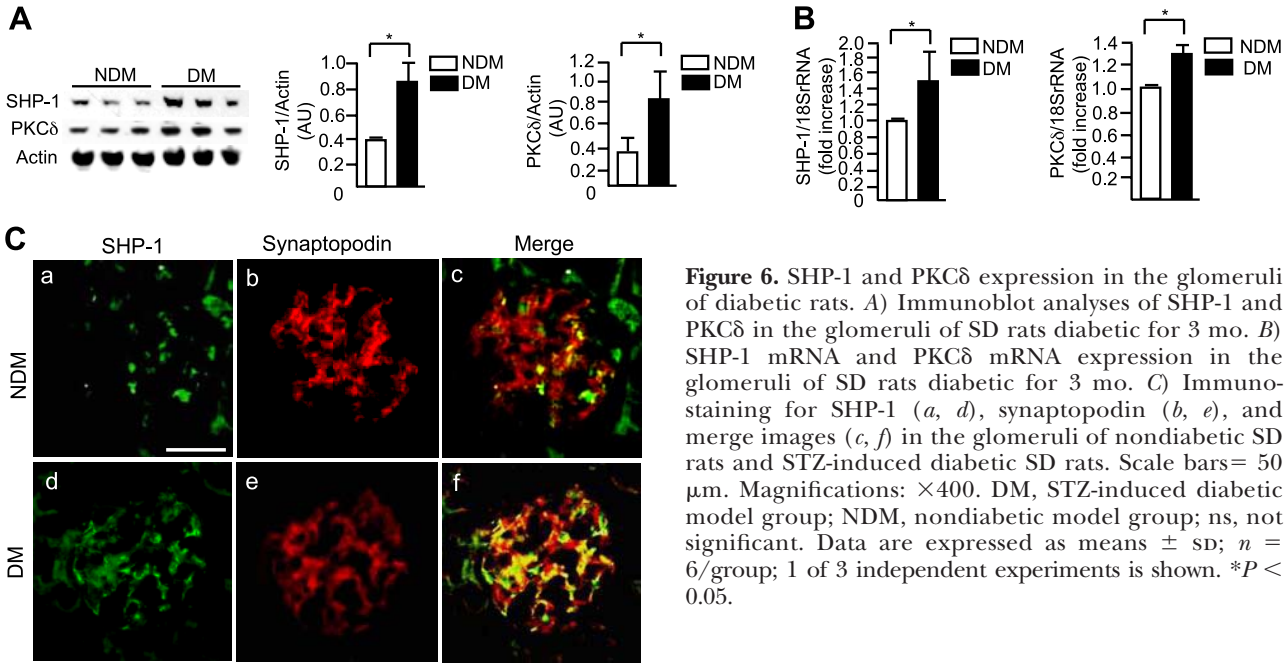

Figure 6. SHP-1 and PKCδ expression in the glomeruli of diabetic rats. *A*) Immunoblot analyses of SHP-1 and PKCδ in the glomeruli of SD rats diabetic for 3 mo. *B*) SHP-1 mRNA and PKCδ mRNA expression in the glomeruli of SD rats diabetic for 3 mo. *C*) Immunostaining for SHP-1 (*a*, *d*), synaptopodin (*b*, *e*), and merge images (*c*, *f*) in the glomeruli of nondiabetic SD rats and STZ-induced diabetic SD rats. Scale bars= 50 μm. Magnifications: ×400. DM, STZ-induced diabetic model group; NDM, nondiabetic model group; ns, not significant. Data are expressed as means ± SD; n = 6/group; 1 of 3 independent experiments is shown. *$P <$ 0.05.

caspase-3 expression were reduced significantly in diabetic *Prkcd*$^{-/-}$ (37±10%) *vs.* diabetic *Prkcd*$^{+/+}$ mice (Fig. 7*C*). Similarly, the levels of TUNEL/nephrin/DAPI triple-positive cell numbers in the renal cortex were elevated in diabetic *Prkcd*$^{+/+}$ mice by 11 ± 3-fold compared to nondiabetic *Prkcd*$^{+/+}$ mice. Again, this increase was reduced significantly in diabetic *Prkcd*$^{-/-}$ (51±16%) *vs.* diabetic *Prkcd*$^{+/+}$ mice (Supplemental Fig. S2*D*).

We evaluated the role of PKCδ activation and the reversibility of SHP-1 mRNA expression in the renal cortex. Expression of PKCδ and SHP-1 mRNA levels increased in parallel in the renal cortex of diabetic *Prkcd*$^{+/+}$ mice after 6 mo of diabetes by 1.7 ± 0.2- and 1.7 ± 0.3-fold, respectively (Supplemental Fig. S2*E*, *F*). In contrast, SHP-1 mRNA expression did not differ in diabetic *Prkcd*$^{-/-}$ mice compared to nondiabetic controls (Supplemental Fig. S2*F*). SHP-1 and p-p38 MAPK protein expression levels were elevated in the renal cortex of diabetic *Prkcd*$^{+/+}$ mice by 2.3 ± 0.5- and 2.7 ± 0.9-fold, respectively (Fig. 7*D* and Supplemental Fig. S2*G*). In contrast, diabetic *Prkcd*$^{-/-}$ mice exhibited no significant changes in SHP-1 or p-p38 MAPK protein expression compared to nondiabetic *Prkcd*$^{-/-}$ mice (Fig. 7*D* and Supplemental Fig. S2*G*). The expression of TGF-β and type IV collagen mRNA was elevated in the renal cortex of diabetic *Prkcd*$^{+/+}$ mice by 1.7 ± 0.3- and 1.8 ± 0.2-fold, respectively (Fig. 7*E*, *F*). This increase was significantly reduced in the renal cortex of diabetic *Prkcd*$^{-/-}$ mice by 31 ± 11 and 27 ± 10%, respectively (Fig. 7*E*, *F*). VEGF expression was elevated in the renal cortex of diabetic *Prkcd*$^{+/+}$ and *Prkcd*$^{-/-}$ mice; however, this increase was significantly reduced in the renal cortex of diabetic *Prkcd*$^{-/-}$ mice by 27 ± 11% (Fig. 7*G*). Albuminuria in diabetic *Prkcd*$^{-/-}$ mice was lower by 39 ± 9%, but not completely prevented, compared to diabetic *Prkcd*$^{+/+}$ mice (Table 2). Kidney and total body ratio were elevated equally by diabetes in *Prkcd*$^{+/+}$ and *Prkcd*$^{-/-}$ mice (Table 2).

DISCUSSION

This study, for the first time, identified and characterized VEGF resistance in the renal glomeruli induced by diabetes. This conclusion is supported by the findings that VEGF-induced p-nephrin was blunted in diabetic

TABLE 2. *Metabolic characteristics of nondiabetic and diabetic* Prkcd$^{+/+}$ *and* Prkcd$^{-/-}$ *mice*

	Prkcd$^{+/+}$		*Prkcd*$^{-/-}$	
Characteristic	NDM	DM	NDM	DM
Number	9	8	6	7
Body weight (g)	38.7 ± 1.4	27.0 ± 1.2*	37.5 ± 2.2	26.4 ± 3.0*
Blood glucose (mg/dl)	127 ± 8	552 ± 46*	125 ± 8	493 ± 103*
rKW/BW(mg/g)	4.8 ± 0.4	10.1 ± 1.5*	4.9 ± 0.2	9.7 ± 0.8*
UAE(μg/d)	1.3 ± 0.4	7.4 ± 2.7*	0.9 ± 0.3	4.5 ± 1.7*,†

NDM, nondiabetic model; DM, diabetic model; rKW/BW, right kidney weight/body weight; UAE, urinary albumin excretion. Data are expressed as means ± SD. *$P < 0.05$ *vs.* NDM *Prkcd*$^{+/+}$ mice, †$P < 0.05$ *vs.* DM *Prkcd*$^{+/+}$ mice.

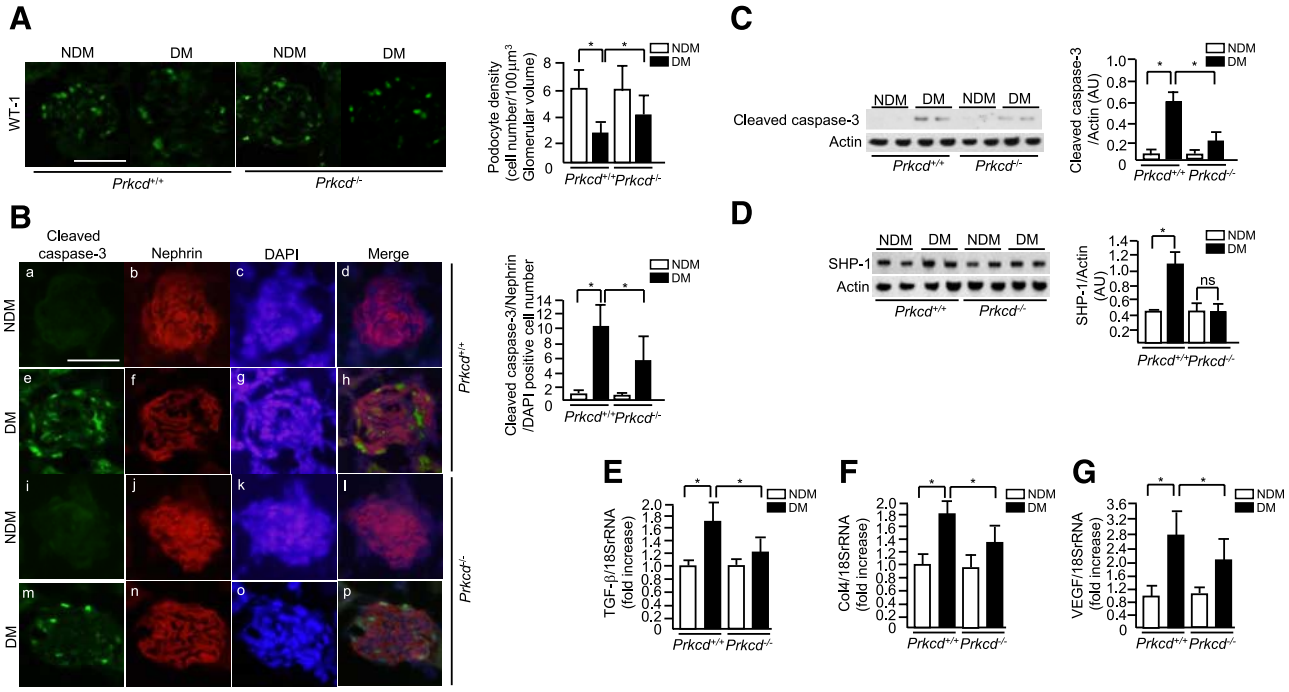

Figure 7. Podocyte apoptosis and SHP-1 expression in diabetic renal cortex of *Prkcd*$^{-/-}$ mice. *A*) Immunostaining and density of WT-1-positive cells per glomerulus in *Prkcd*$^{+/+}$ and *Prkcd*$^{-/-}$ mice. *B*) Immunostaining for cleaved caspase-3 (*a*, *e*, *i*, *m*), nephrin (*b*, *f*, *j*, *n*), DAPI (*c*, *g*, *k*, *o*), and merge images (*d*, *h*, *l*, *p*) in the glomeruli and cleaved caspase-3/nephrin/DAPI triple-positive cells per glomerulus in *Prkcd*$^{+/+}$ and *Prkcd*$^{-/-}$ mice. *C*) Representative immunoblots of cleaved caspase-3 from renal cortex. *D*) Immunoblot analyses of SHP-1 in renal cortex of nondiabetic mice and diabetic *Prkcd*$^{+/+}$ and *Prkcd*$^{-/-}$ mice. *E–G*) mRNA expression of TGF-β (*E*), Col4 (*F*), and VEGF (*G*) in renal cortex of nondiabetic mice and diabetic *Prkcd*$^{+/+}$ mice. Scale bars= 50 μm. Magnifications: ×400. DM, STZ-induced diabetic model group; NDM, nondiabetic model group; ns, not significant. Data are expressed as means ± SD; n = 6–9/group; 1 of 3 independent experiments is shown. *$P < 0.05$.

rats and in cultured podocytes exposed to media containing high glucose concentrations. At low concentrations of VEGF, even p-Akt levels were decreased in the glomeruli of diabetic rats. Thus, for the first time we have evidence that the VEGF signaling pathway in podocytes, to a lesser extent endothelial cells, and glomeruli are inhibited selectively by diabetes due to hyperglycemia. This is the likely explanation for the compensatory elevation of VEGF levels in the glomeruli of diabetic animals and patients, which have been reported to be increased in kidney biopsies of patients with type 2 diabetes at all stages of nephropathy (21).

The mechanism for diabetes-induced VEGF resistance in the glomeruli appears to be related to PKC activation. Our results suggest that the persistent activation of PKCδ is upstream to at least two different pathways, which could be responsible for podocyte apoptosis induced by hyperglycemia. Activation of PKCδ and other PKC isoforms has been reported in the glomeruli and other vascular tissues in patients and animals with diabetes (8). Among the PKC isoforms, which were activated in the podocytes, PKCδ appears to be mainly responsible for its apoptosis and only partially affects the expression of VEGF, TGFβ, and type IV collagen. It is likely that the activation of PKCα/β isoforms may be responsible for other renal effects, especially in the endothelial cells. Menne *et al.* (22) reported that diabetes in PKCα-null mice had less albuminuria and VEGF expression in the kidney but did not improve TGFβ and renal hypertrophy. Quack *et al.* (23) showed that nephrin endocytosis can be regulated by PKCα. Diabetes-induced PKCβ activation has been reported in all glomerular cells (24). However, it is very likely that PKCδ activation is primarily responsible for the increase in podocyte apoptosis rather than PKCα/β, since PKCδ activation can induce apoptosis of various types of cells, including cardiomyocytes (25), neuronal cells (26), tubular cells (27), and endothelial cells (28). In addition, evidence indicates that PKCδ could provide proapoptosis signal, since it is a substrate for caspase-3 (29). In this study, the direct effect of PKC activation on podocyte apoptosis appears to be PKCδ selective, since overexpression of PKCα and β did not enhance apoptosis either in low- or high-glucose medium.

In the podocyte, the increase in PKCδ appears to mediate its apoptotic actions by activating p38 MAPK, which has been previously reported in the glomeruli of diabetic animals and mesangial cells exposed to elevated glucose levels (30). p38 MAPK activation in the podocyte can induce at least two different pathways to accelerate apoptosis. First, a known mechanism involves hyperglycemia-induced increased production of reactive oxygen species, possibly due to activation of oxidases, which leads to NF-κB activity induction, as shown by multiple previous reports (20), and is clearly important partly for podocyte apoptosis. Our study suggests that a novel second and equally important pathway for hyperglycemia to induce podocyte apoptosis is SHP-1 induction leading to the selective inhibition

of VEGFR-2, which paralleled the time course of PKCδ and SHP-1 activation at 1 mo and reached maximum at 3 mo (8). This appears to be a selective effect of SHP-1, since the activation of IGF-1 or EGF signaling was not inhibited in podocyte cultures when exposed to glucose elevation in the medium. Interestingly, SHP-1 has been reported to down-regulate several tyrosine kinase receptors, including VEGFR-2, PDGFR-β, insulin receptors, and EGF receptors (31, 32). However, the actions of SHP-1 have not been reported in podocytes. This is the first report showing that SHP-1 activation by diabetes and glucose elevation can inhibit VEGF action in podocytes. Previous *in vivo* models of SHP-1 mutation in mice leads to severe disruptions resulting in death several weeks after birth, which make prolonged studies not feasible at this time (33). Thus, it is possible that activation of SHP-1 could deactivate other tyrosine kinase receptors in the podocytes. These studies are in progress.

The results from the *Prkcd*$^{-/-}$ mice support the importance of PKCδ activation in stimulating apoptotic signal in the glomeruli, which correlates with lack of changes in p38 activation and SHP-1 expression. It is likely that PKCδ activation is responsible for only some of the pathologies observed in the kidneys of diabetic mice. For example, the increase in VEGF expression and albuminuria appears to be improved, but not prevented, whereas renal hypertrophy was not changed. These studies clearly suggest that PKCδ plays an important role in mediating podocyte apoptosis and possibly of renal endothelial cell dysfunction, indirectly.

Some reports have suggested that inhibition of VEGF-A had beneficial effects against diabetic renal injuries (34). Schrijvers *et al.* (35) reported that treatment with VEGF-A antibodies did not improve diabetic renal abnormalities in G-K rats. Reports by Quaggin and colleagues (7, 36) clearly showed that VEGF-A is necessary for forming and maintaining the glomerular filtration barrier. Loss of a single VEGF-A allele in podocytes leads to endotheliosis, glomerulosclerosis, renal failure, and death (7). Clinically, the use of anti-VEGF antibody resulted in varying degrees of proteinuria, hypertension, and renal failure (36). Our results support the idea that appropriate levels of VEGF are needed to maintain the survival and proper function of the glomeruli. Treatment of diabetic nephropathy with anti-VEGF may cause glomerular pathology if proper VEGF levels in the glomeruli are not maintained.

Our studies clearly showed that VEGF-A increased p-Erk both *in vivo* and *in vitro*, and this effect may be decreased by diabetes. Elevation of p-Erk is associated with increasing extracellular matrix in mesangial cells (37, 38), which can contribute to glomerular pathology. However, it is not clear whether VEGF activation is contributing to extracellular matrix thickening, since VEGF, a potent mitogen for endothelial cell proliferation, usually *via* pERK activation, enhances basement membrane degradation during the induction of cell replication. Further studies will be needed to determine the effect of the loss of VEGF activation on pERK in endothelial cells or podocytes in diabetes.

The importance of VEGF actions on podocytes has been questioned since Sison *et al.* (9) reported that podocytes in culture did not express VEGFR-2, and selective KO deletion of VEGFR-2 in the podocytes did not delay significant pathology. In this study, double immunostaining analysis of glomeruli using nephrin and VEGFR-2 antibody showed that VEGFR-2 was detected in the podocyte *in vivo* (Supplemental Fig. S2*A*). In other reports, several groups have detected VEGFR-2 on podocytes *in vivo* by immunostaining or immunogold techniques in animals and human samples (39). In cultured podocytes, our studies clearly demonstrated that VEGFR-2 is present and can elicit cellular effects. Thus, VEGFR-2 receptors may exist in renal podocytes depending on the podocytes' origin. However, the biological significance of VEGFR-2 on the podocyte is unclear. It is possible that the ambient need to preserve the function of glomerular endothelial cells can be supported by constitutive production of VEGF from the podocyte without its paracrine actions in unstressed environments. However, with endothelial dysfunction as in diabetes, an additional need for VEGF could remain due to parallel endothelial VEGF resistance (15). VEGFR-2 on podocytes may play a role to provide the additional requirement of VEGF under stress conditions. Thus, the manifestation of VEGF resistance on podocytes and endothelial cells could contribute to glomerular dysfunction in diabetes if further studies can confirm its pathophysiological importance. These findings support the need for effective therapies for diabetic nephropathy that can neutralize the effects of the toxic metabolites of glucose and their inhibitory actions on protective factors such as VEGF due to SHP-1 activation. FJ

The authors thank Dr. Hillary Keenan for the discussions on the statistical analysis and Ms. Patti Muehter for excellent assistance with manuscript preparation. This work is supported by grants to G.L.K. from the U.S. National Institutes of Health/National Eye Institute (EY016150). A.M. is the recipient of a Research Fellowship (Manpei Suzuki Diabetes Foundation, Kanzawa Medical Research Foundation, Novartis Foundation, Japan). This project has been supported by Diabetes and Endocrinology Research Center grant P30DK036836.

REFERENCES

1. Remuzzi, G., Benigni, A., and Remuzzi, A. (2006) Mechanisms of progression and regression of renal lesions of chronic nephropathies and diabetes. *J. Clin. Invest.* **116,** 288–296
2. Ellis, E. N., Steffes, M. W., Chavers, B., and Mauer, S. M. (1987) Observations of glomerular epithelial cell structure in patients with type I diabetes mellitus. *Kidney Int.* **32,** 736–741
3. Gubler, M. C. (2003) Podocyte differentiation and hereditary proteinuria/nephrotic syndromes. *J. Am. Soc. Nephrol.* **14**(Suppl. 1), S22–S26
4. Pagtalunan, M. E., Miller, P. L., Jumping-Eagle, S., Nelson, R. G., Myers, B. D., Rennke, H. G., Coplon, N. S., Sun, L., and Meyer, T. W. (1997) Podocyte loss and progressive glomerular injury in type II diabetes. *J. Clin. Invest.* **99,** 342–348
5. (1998) Intensive blood-glucose control with sulphonylureas or insulin compared with conventional treatment and risk of complications in patients with type 2 diabetes (UKPDS 33). UK Prospective Diabetes Study (UKPDS) Group. *Lancet* **352,** 837–853

6. Stadtman, E. R. (1992) Protein oxidation and aging. *Science* **257,** 1220–1224
7. Eremina, V., Sood, M., Haigh, J., Nagy, A., Lajoie, G., Ferrara, N., Gerber, H. P., Kikkawa, Y., Miner, J. H., and Quaggin, S. E. (2003) Glomerular-specific alterations of VEGF-A expression lead to distinct congenital and acquired renal diseases. *J. Clin. Invest.* **111,** 707–716
8. Geraldes, P., Hiraoka-Yamamoto, J., Matsumoto, M., Clermont, A., Leitges, M., Marette, A., Aiello, L. P., Kern, T. S., and King, G. L. (2009) Activation of PKC-delta and SHP-1 by hyperglycemia causes vascular cell apoptosis and diabetic retinopathy. *Nat. Med.* **15,** 1298–1306
9. Sison, K., Eremina, V., Baelde, H., Min, W., Hirashima, M., Fantus, I. G., and Quaggin, S. E. (2010) Glomerular structure and function require paracrine, not autocrine, VEGF-VEGFR-2 signaling. *J. Am. Soc. Nephrol.* **21,** 1691–1701
10. Leitges, M., Mayr, M., Braun, U., Mayr, U., Li, C., Pfister, G., Ghaffari-Tabrizi, N., Baier, G., Hu, Y., and Xu, Q. (2001) Exacerbated vein graft arteriosclerosis in protein kinase Cdelta-null mice. *J. Clin. Invest.* **108,** 1505–1512
11. Tryggvason, K., and Kouvalainen, K. (1975) Number of nephrons in normal human kidneys and kidneys of patients with the congenital nephrotic syndrome. A study using a sieving method for counting of glomeruli. *Nephron* **15,** 62–68
12. Mundel, P., Reiser, J., Zuniga Mejia Borja, A., Pavenstadt, H., Davidson, G. R., Kriz, W., and Zeller, R. (1997) Rearrangements of the cytoskeleton and cell contacts induce process formation during differentiation of conditionally immortalized mouse podocyte cell lines. *Exp. Cell Res.* **236,** 248–258
13. Mima, A., Ohshiro, Y., Kitada, M., Matsumoto, M., Geraldes, P., Li, C., Li, Q., White, G. S., Cahill, C., Rask-Madsen, C., and King, G. L. (2011) Glomerular-specific protein kinase C-beta-induced insulin receptor substrate-1 dysfunction and insulin resistance in rat models of diabetes and obesity. *Kidney Int.* **79,** 883–896
14. Suzuma, K., Takahara, N., Suzuma, I., Isshiki, K., Ueki, K., Leitges, M., Aiello, L. P., and King, G. L. (2002) Characterization of protein kinase C beta isoform's action on retinoblastoma protein phosphorylation, vascular endothelial growth factor-induced endothelial cell proliferation, and retinal neovascularization. *Proc. Natl. Acad. Sci. U. S. A.* **99,** 721–726
15. Naruse, K., Rask-Madsen, C., Takahara, N., Ha, S. W., Suzuma, K., Way, K. J., Jacobs, J. R., Clermont, A. C., Ueki, K., Ohshiro, Y., Zhang, J., Goldfine, A. B., and King, G. L. (2006) Activation of vascular protein kinase C-beta inhibits Akt-dependent endothelial nitric oxide synthase function in obesity-associated insulin resistance. *Diabetes* **55,** 691–698
16. Weibel, E. R., and Gomez, D. M. (1962) A principle for counting tissue structures on random sections. *J. Appl. Physiol.* **17,** 343–348
17. Steffes, M. W., Schmidt, D., McCrery, R., and Basgen, J. M. (2001) Glomerular cell number in normal subjects and in type 1 diabetic patients. *Kidney Int.* **59,** 2104–2113
18. Busik, J. V., Mohr, S., and Grant, M. B. (2008) Hyperglycemia-induced reactive oxygen species toxicity to endothelial cells is dependent on paracrine mediators. *Diabetes* **57,** 1952–1965
19. Igarashi, M., Wakasaki, H., Takahara, N., Ishii, H., Jiang, Z. Y., Yamauchi, T., Kuboki, K., Meier, M., Rhodes, C. J., and King, G. L. (1999) Glucose or diabetes activates p38 mitogen-activated protein kinase via different pathways. *J. Clin. Invest.* **103,** 185–195
20. Romeo, G., Liu, W. H., Asnaghi, V., Kern, T. S., and Lorenzi, M. (2002) Activation of nuclear factor-kappaB induced by diabetes and high glucose regulates a proapoptotic program in retinal pericytes. *Diabetes* **51,** 2241–2248
21. Hohenstein, B., Hausknecht, B., Boehmer, K., Riess, R., Brekken, R. A., and Hugo, C. P. (2006) Local VEGF activity but not VEGF expression is tightly regulated during diabetic nephropathy in man. *Kidney Int.* **69,** 1654–1661
22. Menne, J., Park, J. K., Boehne, M., Elger, M., Lindschau, C., Kirsch, T., Meier, M., Gueler, F., Fiebeler, A., Bahlmann, F. H., Leitges, M., and Haller, H. (2004) Diminished loss of proteoglycans and lack of albuminuria in protein kinase C-alpha-deficient diabetic mice. *Diabetes* **53,** 2101–2109
23 Quack, I., Woznowski, M., Potthoff, S. A., Palmer, R., Koenigshausen, E., Sivritas, S., Schiffer, M., Stegbauer, J., Vonend, O., Rump, L. C., and Sellin, L. Protein kinase C alpha (PKC α) mediates β-arrestin2-dependent nephrin endocytosis in hyperglycemia. *J. Biol. Chem.* **15,** 12959–12970
24. Koya, D., Jirousek, M. R., Lin, Y. W., Ishii, H., Kuboki, K., and King, G. L. (1997) Characterization of protein kinase C beta isoform activation on the gene expression of transforming growth factor-beta, extracellular matrix components, and prostanoids in the glomeruli of diabetic rats. *J. Clin. Invest.* **100,** 115–126
25. Tanaka, M., Terry, R. D., Mokhtari, G. K., Inagaki, K., Koyanagi, T., Kofidis, T., Mochly-Rosen, D., and Robbins, R. C. (2004) Suppression of graft coronary artery disease by a brief treatment with a selective epsilonPKC activator and a deltaPKC inhibitor in murine cardiac allografts. *Circulation* **110,** II194–II199
26. Kim, Y. H., Kim, Y. S., Park, C. H., Chung, I. Y., Yoo, J. M., Kim, J. G., Lee, B. J., Kang, S. S., Cho, G. J., and Choi, W. S. (2008) Protein kinase C-delta mediates neuronal apoptosis in the retinas of diabetic rats via the Akt signaling pathway. *Diabetes* **57,** 2181–2190
27. Li, X., Pabla, N., Wei, Q., Dong, G., Messing, R. O., Wang, C. Y., and Dong, Z. (2010) PKC-delta promotes renal tubular cell apoptosis associated with proteinuria. *J. Am. Soc. Nephrol.* **21,** 1115–1124
28. Shizukuda, Y., Helisch, A., Yokota, R., and Ware, J. A. (1999) Downregulation of protein kinase cdelta activity enhances endothelial cell adaptation to hypoxia. *Circulation* **100,** 1909–1916
29. Emoto, Y., Manome, Y., Meinhardt, G., Kisaki, H., Kharbanda, S., Robertson, M., Ghayur, T., Wong, W. W., Kamen, R., Weichselbaum, R., and Kufe, D. (1995) Proteolytic activation of protein kinase C delta by an ICE-like protease in apoptotic cells. *EMBO J.* **14,** 6148–6156
30. Wilmer, W. A., Dixon, C. L., and Hebert, C. (2001) Chronic exposure of human mesangial cells to high glucose environments activates the p38 MAPK pathway. *Kidney Int.* **60,** 858–871
31. Brownlee, M. (2001) Biochemistry and molecular cell biology of diabetic complications. *Nature* **414,** 813–820
32. Dubois, M. J., Bergeron, S., Kim, H. J., Dombrowski, L., Perreault, M., Fournes, B., Faure, R., Olivier, M., Beauchemin, N., Shulman, G. I., Siminovitch, K. A., Kim, J. K., and Marette, A. (2006) The SHP-1 protein tyrosine phosphatase negatively modulates glucose homeostasis. *Nat. Med.* **12,** 549–556
33. Shultz, L. D., Schweitzer, P. A., Rajan, T. V., Yi, T., Ihle, J. N., Matthews, R. J., Thomas, M. L., and Beier, D. R. (1993) Mutations at the murine motheaten locus are within the hematopoietic cell protein-tyrosine phosphatase (Hcph) gene. *Cell* **73,** 1445–1454
34. De Vriese, A. S., Tilton, R. G., Stephan, C. C., and Lameire, N. H. (2001) Vascular endothelial growth factor is essential for hyperglycemia-induced structural and functional alterations of the peritoneal membrane. *J. Am. Soc. Nephrol.* **12,** 1734–1741
35. Schrijvers, B. F., De Vriese, A. S., Tilton, R. G., Van de Voorde, J., Denner, L., Lameire, N. H., and Flyvbjerg, A. (2005) Inhibition of vascular endothelial growth factor (VEGF) does not affect early renal changes in a rat model of lean type 2 diabetes. *Horm. Metab. Res.* **37,** 21–25
36. Eremina, V., Jefferson, J. A., Kowalewska, J., Hochster, H., Haas, M., Weisstuch, J., Richardson, C., Kopp, J. B., Kabir, M. G., Backx, P. H., Gerber, H. P., Ferrara, N., Barisoni, L., Alpers, C. E., and Quaggin, S. E. (2008) VEGF inhibition and renal thrombotic microangiopathy. *N. Engl. J. Med.* **358,** 1129–1136
37. Lin, C. L., Wang, F. S., Kuo, Y. R., Huang, Y. T., Huang, H. C., Sun, Y. C., and Kuo, Y. H. (2006) Ras modulation of superoxide activates ERK-dependent fibronectin expression in diabetes-induced renal injuries. *Kidney Int.* **69,** 1593–1600
38. Toyoda, M., Suzuki, D., Honma, M., Uehara, G., Sakai, T., Umezono, T., and Sakai, H. (2004) High expression of PKC-MAPK pathway mRNAs correlates with glomerular lesions in human diabetic nephropathy. *Kidney Int.* **66,** 1107–1114
39. Ku, C. H., White, K. E., Dei Cas, A., Hayward, A., Webster, Z., Bilous, R., Marshall, S., Viberti, G., and Gnudi, L. (2008) Inducible overexpression of sFlt-1 in podocytes ameliorates glomerulopathy in diabetic mice. *Diabetes* **57,** 2824–2833

Received for publication January 2, 2012.
Accepted for publication April 2, 2012.